Strain ratchetting of titanium upon reversible alloying with hydrogen

M. Frary , C. Schuh & D. C. Dunand

Strain ratchetting of titanium upon reversible alloying with hydrogen

M. FRARY, C. SCHUH and D. C. DUNAND*

Department of Materials Science and Engineering, Northwestern University,
Evanston, Illinois, 60208, USA

ABSTRACT

During cyclic hydrogen charging (e.g., in metal–hydride systems), internal stresses and strains can be developed due to lattice swelling and/or phase transformation (e.g., allotropic transformation or hydride precipitation). We examine macroscopic plastic deformation due to such internal stresses (*strain ratchetting*) in the Ti–H system, where gaseous hydrogen is alloyed with Ti, causing the Ti α–β allotropic transformation, and subsequently removed, producing the β–α transformation. Cyclic hydrogen charging is found to cause macroscopic plastic shrinkage strains in directions normal to the hydrogen concentration gradient. Furthermore, increasing the charging time leads to larger ratchetting strains. A simple adaptation of diffusion theory is used to describe the kinetics of strain evolution, and the contributions to total ratchetting from both the α–β phase transformation and the lattice swelling strains are quantified.

§1. INTRODUCTION

Materials and structures subjected to thermal excursions frequently develop thermal mismatch stresses due to thermal gradients or thermal expansion mismatch between, for example, coexisting phases. When these mismatch stresses are sufficient to produce plastic deformation (i.e., by yield or creep), an irreversible macroscopic strain increment can develop after a fully reversed thermal cycle, as observed after as little as one cycle in SiC whisker-reinforced aluminium alloys (in which the phases have a thermal-expansion mismatch) (Nakanishi *et al.* 1990, Hall and Patterson 1991) and in zinc bicrystals (in which the adjacent grains have a thermal expansion mismatch) (Burke and Turkalo 1952). This phenomenon, called *thermal ratchetting*, is observed also in structures with thermal gradients, for example in pipes with oscillating liquid levels (Bree 1967, Ponter and Cocks 1984). Ratchetting may further occur due to a solid–solid phase transformation; when a phase boundary moves through a specimen during transformation, there is a tendency for the specimen to retain the dimensions of the stronger phase in the directions tangential to the boundary (Stobo 1960). Ratchetting caused by thermally cycling a material around its allotropic transformation temperature has been studied primarily with regard to uranium (Buckley *et al.* 1958, Stobo 1960, Young *et al.* 1960, Greenwood and Johnson 1962), for its implications in nuclear reactors.

---

*Author for correspondence. e-mail: dunand@northwestern.edu

Although ratchetting is typically a product of thermal cycling, it can result from any source of internal stress. The cycling of any intensive thermodynamic variable (i.e., temperature, pressure, or chemical composition) may produce mismatch stresses between adjacent phases, anisotropic grains of the same phase, or may trigger a solid-state phase transformation that produces ratchetting. Indeed, microscopic plastic deformation due to chemical composition changes has been observed in several metal–hydride systems (Nb–H (Birnbaum *et al.* 1976, Schober and Wenzel 1978, Makenas and Birnbaum 1980, Balasubramaniam 1993), Zr–H (Bailey 1963, Puls 1981), and TiAl–H (Paton *et al.* 1971)) upon the addition of hydrogen and subsequent precipitation of a hydride phase. During precipitation, the less-dense hydride phase is restricted from freely expanding by the surrounding matrix, which plastically deforms to accommodate the volume change. Transmission electron microscopy studies of precipitating hydrides suggest that the formation of interfacial dislocations and punching of prismatic dislocation loops accommodate the transformation volume mismatch (Schober 1973, Birnbaum *et al.* 1976). These plastic deformation processes are not generally reversible, and must be present both on hydride precipitation and on reversion (Birnbaum *et al.* 1976). Many studies (Lee *et al.* 1980, Makenas and Birnbaum 1980, Earmme *et al.* 1981, Puls 1981, Balasubramaniam 1993) have been devoted to observing and modelling the microscopic deformation that attends hydride precipitation.

The purpose of the present work is to demonstrate macroscopic ratchetting strains upon cyclic alloying/dealloying of titanium with hydrogen. Experiments are conducted at 860°C, where diffusion of gaseous hydrogen into titanium is rapid and induces the allotropic phase transformation of Ti (α(HCP) → β(BCC)). Although this transformation does not involve hydride precipitation, it can serve as a useful analogue for those more complex phase transformations. Macroscopic shape change due to cyclic hydrogen charging may have significant implications for the long term stability of hydrogen storage systems (i.e., metal–hydride systems), as well as for 'thermohydrogen processing' of titanium (Froes and Eylon 1990, Senkov *et al.* 1996), in which hydrogen is added to titanium or titanium alloys as a temporary alloying element producing the β-phase for improved forming characteristics. Alternatively, this effect may be exploited to intentionally produce large strains by transformation superplasticity (P. Zwigl and D. C. Dunand, unpublished).

§ 2. Experimental procedures

The experimental specimens were cylinders of high purity titanium (99.99%, from Alfa Aesar, Ward Hill, MA), with diameter 3.175 mm and length approximately 10 mm. All experiments were carried out in a quenching dilatometer (from MMC, Westbury, NY), which allowed for measurement of small strains (0.1 μm resolution, 0.001% for 10 mm long specimen), selection of test atmosphere (vacuum or Ar/H_2 gas mixture) and closed-loop induction heating with temperature control within ±2 K, monitored by an R-type thermocouple spot-welded to the specimen surface.

Each specimen was subjected to either a thermal or chemical excursion to investigate macroscopic strain development. The thermal or chemical history for each type of experiment is shown schematically on a section of the Ti–H phase diagram in figure 1, and described in detail below.
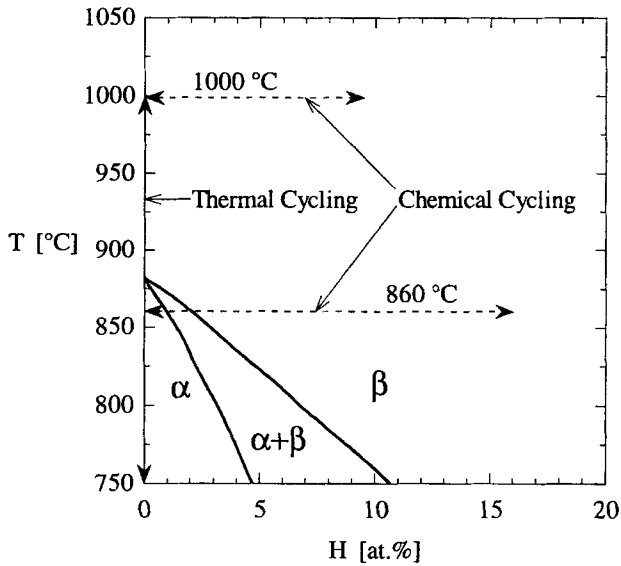
Figure 1. Selected portion of the Ti–H phase diagram after Lewkowicz (1996), showing thermal and composition ranges used in the experiments.

2.1. *Thermal cycling experiments*

Thermal cycling experiments about the Ti α–β allotropic transformation at 882°C (McQuillan 1950) were performed on a single specimen, to establish the thermal ratchetting behaviour of hydrogen-free Ti as a baseline for the chemical cycling studies. The specimen was heated to 1000°C (in the β-field) in 300 s, held at that temperature for 1200 s, then cooled to room temperature (in the α-field) in 600 s. Two such thermal cycles were completed on the same specimen in a vacuum of 10^{-5} Torr, without any external stress (the dilatometer platens were not in contact with the specimen). The plastic strain accumulated after each cycle was assessed by measuring the specimen length with a micrometer at room temperature before and after each cycle. This technique allowed a strain resolution of 1.4 μm, or 0.014% for a specimen 10 mm long.

2.2. *Chemical cycling experiments*

In each chemical cycling experiment, the specimen was heated rapidly (in 120–600 s) to a temperature of 860°C (unless stated otherwise) and maintained at that temperature during subsequent cyclic hydrogen alloying/dealloying. Once the specimen was at temperature under vacuum (10^{-5} Torr), the chamber was filled with 4% H_2 in Ar gas at a hydrogen partial pressure of $P_{H_2} = 38.7$ Torr to induce the α → β transformation. After transforming, the Ti–H alloy approaches equilibrium as given by Sievert's Law (McQuillan 1950):

$$\log P_{H_2} = 2\log c_{eq} + 7.343 - 4720/T, \tag{1}$$

where c_{eq} is the equilibrium dissolved hydrogen concentration in at.% and T is the temperature in kelvins. Under the experimental conditions described above, the equilibrium concentration of hydrogen in β-Ti is calculated from equation (1) as $c_{eq} = 16.0$ at.%. This concentration is sufficient to insure a complete α → β trans-

formation (figure 1), without formation of hydride phases (McQuillan 1950, Lewkowicz 1996). Unlike thermal cycling, which induces the allotropic α–β transformation at a single temperature, chemical cycling involves a traversal of the two-phase α + β field (figure 1).

After hydrogen charging for 150, 300, 600, 900, or 1200 s at 860°C, the vacuum was re-established for 1500 s to remove the dissolved hydrogen from the specimen. Only a single chemical cycle was performed on any specimen. Two types of chemical cycling experiment were performed, as described in the following.

First, in dilatometric experiments, specimens were placed horizontally in the dilatometer in contact with two quartz platens, allowing *in situ* measurement of the specimen length change (with a linear voltage-displacement transducer (LVDT) in the cold zone) as a function of time during both the H charging and discharging half-cycles. While the compressive stress due to platen contact was too small to be measured, these contact stresses had no effect on hydrogen charging or strain development, as verified through a second series of experiments, as described below, and discussed in more detail in later sections.

Second, in contact-free experiments, specimens were positioned in the dilatometer such that there was no contact with the platens, assuring no external biasing stresses that might influence ratchetting deformation. Because of this arrangement, the specimen length could no longer be monitored with an LVDT, so the macroscopic strain increment after each H cycle was assessed by micrometer measurements at room temperature, as for the thermal cycling experiments.

In addition to the chemical cycling experiments at 860°C, one specimen was also tested at 1000°C, with half-cycles of 1200 s and 1500 s duration for charging and discharging, respectively. At this temperature, with $P_{H_2} = 38.7$ Torr, equation (1) gives the equilibrium hydrogen concentration $c_{eq} = 9.5$ at.%. Again, hydride phases are not expected, and the test temperature is such that the α–β transformation does not occur during the hydrogen cycle (figure 1).

§3. RESULTS

3.1. *Thermal cycling*

The ratchetting strain resulting from each thermal cycle from 25°C to 1000°C (across the α–β transus at 882°C) was $\Delta\varepsilon_{r,thermal} = 0.05 \pm 0.014\%$. The positive sign of the strain denotes a ratchetting length increase, consistent with previous work on thermal cycling of titanium (Furushiro *et al.* 1987). The fact that ratchetting was reproducible indicates that the strain after the first cycle is not due to relaxation of internal stresses from extrusion or machining. The additive nature of thermal ratchetting strains is consistent with the work on uranium by Buckley *et al.* (1958).

3.2. *Chemical cycling*

3.2.1. *Dilatometric experiments*

The strain history measured during a single hydrogen cycle in the dilatometric experiments is shown in figure 2. The kinetics of strain evolution during charging are consistent for all experiments, as evidenced by the near overlap of all experimental curves. The total strain developed during hydrogen charging, $\Delta\varepsilon_c$, has a maximum value of about 0.37%, observed after charging for 600, 900, or 1200 s. Similarly, the total strain recovered on hydrogen discharging, $\Delta\varepsilon_d$, has a maximum absolute value
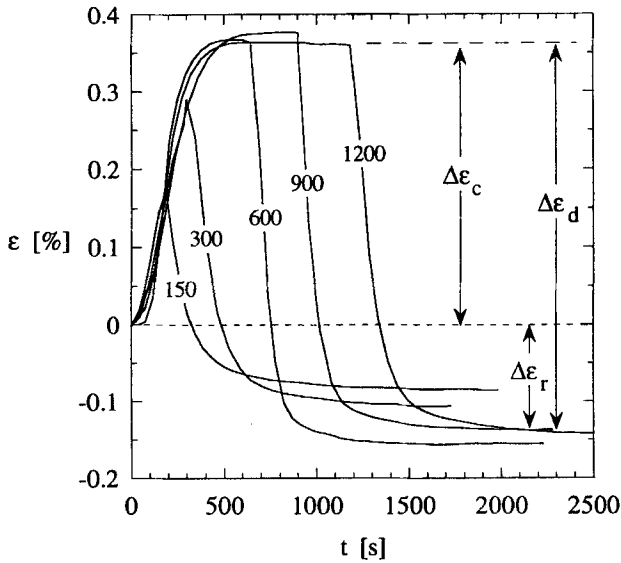
Figure 2. Strain history of titanium specimens during dilatometric hydrogen cycling experiments at 860°C. Each curve is labelled with the charging time, t_c, in seconds, and the strain of charging ($\Delta\varepsilon_c$), strain of discharging ($\Delta\varepsilon_d$), and chemical ratchetting strain ($\Delta\varepsilon_r$) are shown schematically for the longest experiment ($t_c = 1200$ s).

of 0.52% for the specimen charged for 600 s. The negative strain remaining after a single cycle is the chemical ratchetting strain, $\Delta\varepsilon_{r,\,chemical} = \Delta\varepsilon_c - \Delta\varepsilon_d$, which has a maximum negative value of -0.15%, obtained after 600 s of charging and 1500 s of discharging.

Figure 3 shows $-\Delta\varepsilon_{r,\,chemical}$ plotted as a function of the hydrogen charging time t_c. The ratchetting shrinkage increases monotonically with t_c up to $t_c \approx 600$ s, above which it reaches a plateau with an absolute value of about 0.15%.

3.2.2. Contact-free experiments

The ratchetting strain, $\Delta\varepsilon_r$, determined from micrometer measurements at room temperature before and after the contact-free chemical cycling experiments, is shown as a function of hydrogen charging time t_c, in figure 3 for comparison with the dilatometry data. The good agreement between the data sets for the two different types of experiment indicates that the very small stress from the dilatometer platens does not markedly alter the measured ratchetting strains.

For the single chemical cycle performed at 1000°C (in the Ti β field), the measured strain after one cycle was $\Delta\varepsilon_{r,\beta} = -0.02 \pm 0.014\%$. Since this experiment involved (a) a thermal cycle between room temperature and 1000°C without dissolved hydrogen and (b) a chemical cycle at 1000°C, the measured strain of -0.02% is composed of a thermal ratchet as well as strain due to the chemical cycle. Taking the thermal ratchetting strain from above ($\Delta\varepsilon_{r,\,thermal} = 0.05 \pm 0.014\%$), the chemical ratchetting strain at 1000°C is found as $\Delta\varepsilon_{r,\,chemical} = \Delta\varepsilon_{r,\beta} - \Delta\varepsilon_{r,\,thermal} = -0.07 \pm 0.02\%$.
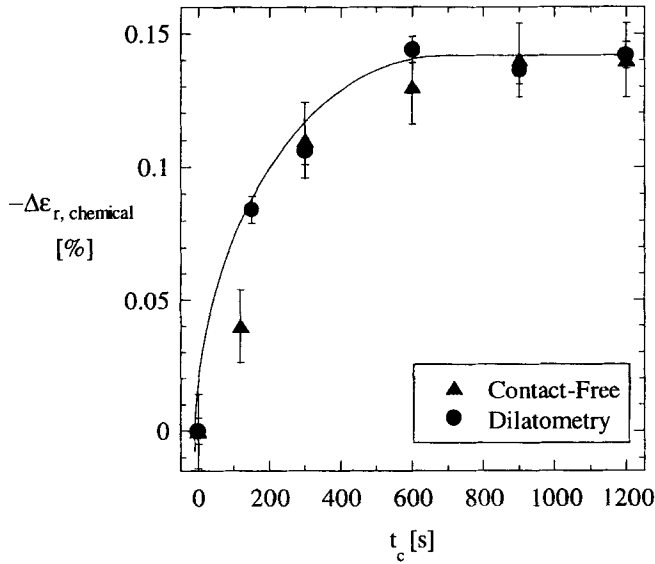
Figure 3. Chemical ratchetting strain, measured in both dilatometric and contact-free hydro-
gen cycling experiments, as a function of hydrogen charging time at 860°C. Trendline
is shown as a visual aid only.

§4. DISCUSSION

4.1. *Thermal cycling*

Ratchetting due to cyclic, thermally induced, allotropic transformation has often
been associated with either (a) large thermal gradients producing a macroscopic
transformation front (Buckley *et al.* 1958, Stobo 1960, Zwigl and Dunand 1998)
or (b) crystallographic texture (Furushiro *et al.* 1987). Either of these anisotropies
may provide a bias for the transformation front to propagate in a preferred direc-
tion. In the present case, thermal gradients may safely be neglected because the
thermal conductivity of titanium is high, the specimens are small, and heating is
performed in a vacuum, with no significant convection condition. Furthermore, the
specimens were sectioned from titanium rods, which tend to have a deformation
texture with hexagonal α-basal planes aligned along the extrusion axis (Lampman
1990). Therefore, the elongation of $\Delta\varepsilon_{r,\ thermal} = 0.05 \pm 0.014\%$ measured after ther-
mal cycles through the α–β transformation is probably due to texture effects of
ratchetting. This conclusion is validated by the work of Furushiro *et al.* (1987),
who measured a ratchetting strain of $\Delta\varepsilon_{r,\ thermal} = 0.035\%$ along the rolling direction
of hot-rolled titanium thermally cycled through the α–β transformation. Since the
textures developed by extrusion and hot-rolling are similar (Lampman 1990), these
results are comparable. It is important to note that in the absence of texture and
macroscopic thermal gradients, no thermal ratchetting would occur.

4.2. *Chemical cycling*

4.2.1. *Kinetics of strain evolution*

The strain histories shown in figure 2 describe the length of the Ti cylinder, which
changes due to distortion of the titanium lattice upon hydrogen absorption (lattice

swelling) as well as the allotropic α–β transformation. Furthermore, because both lattice swelling and transformation are dependent on hydrogen concentration, strain gradients are undoubtedly present during chemical cycling, leading to additional elastic and/or plastic strain mismatch along the diameter of the cylinder.

Although the measured strain evolution is thus composed of several contributions, there is an intrinsic asymmetry in the chemical cycles which simplifies the subsequent analysis, as discussed in the following. As the $\alpha \rightarrow \beta$ transformation begins with the addition of hydrogen, the outer surface of the cylinder first transforms to β-Ti. The much weaker β-Ti phase (Frost and Ashby 1982) is then plastically deformed by the stronger α-Ti core as the transformation progresses toward the cylinder centre. Because the β phase is unconstrained at the cylinder surface, it is able to deform plastically to accommodate the macroscopic shape of the α phase. Since the shell of β-Ti has an elevated hydrogen concentration (relative to the α-Ti), and therefore has a lower density than α-Ti, plastic deformation tends to shorten the shell along its axis, producing a negative ratchetting strain, $\Delta\varepsilon_{r,\ chemical}$.

Upon discharging, however, the situation is quite different; as the hydrogen diffuses out of the cylinder, a shell of α-Ti forms around the edge of the cylinder, with a β-Ti core remaining in the centre. Because the α-Ti shell is strong compared with the β-Ti core, it prevents the β core from deforming plastically. We then assume that strain mismatch between the coexisting phases is not accommodated by plastic deformation of the β phase, but by elastic deformation of both phases. It follows from this model that ratchetting strains develop only on the charging half of the chemical cycle, and that the length changes measured during discharging may be explained simply as the de-swelling of the β lattice upon the diffusion of hydrogen out of the cylinder.

This assumption is employed in the following sections, in which the experimental data are considered in terms of diffusion theory. The goal of this analysis is to describe the kinetics of hydrogen charging and discharging in an approximate manner, so that the propagation of the α–β phase transformation front may be determined, and the respective contributions of phase transformation and lattice swelling to ratchetting assessed.

4.2.1.1. *Hydrogen diffusion during discharging.* Because ratchetting occurs during hydrogen charging, the strain evolution observed on charging (figure 2) is composed of lattice swelling, transformation, and ratchetting strains, making an analytical description difficult. Conversely, the strain history during discharging is assumed to be due only to swelling and transformation, as described above. In this section, we consider the kinetics of diffusion-limited hydrogen discharging for comparison with the experimental data using the three following assumptions.

(i)　By neglecting end effects, the problem reduces to cylindrical symmetry for which Fick's second law of diffusion is (Crank 1975)

$$\frac{\partial c}{\partial t} = \frac{1}{r} \frac{\partial}{\partial r} \left(rD \frac{\partial c}{\partial r} \right), \tag{2}$$

where D is the diffusivity of hydrogen in titanium, t is time and r is the radial coordinate. Trapping of hydrogen internally by vacancies and dislocations (Makhlouf and Sisson 1991) is neglected.

(ii)　At the experimental temperature of 860°C, the trace diffusivities of H in α-Ti $(D_\alpha = 7.0176 \times 10^{-5}\,cm^2\,s^{-1})$ and in β-Ti $(D_\beta = 1.1012 \times 10^{-4}\,cm^2\,s^{-1})$

differ by a factor of only about 1.5 (Lewkowicz 1996). Therefore, the local discontinuity in diffusivity at the transformation front may be neglected, and a single diffusivity value employed in the calculations. D is taken to be concentration independent, as shown in Wasilewski and Kehl (1954). The controlling value of D, as well as errors arising from this assumption, will be discussed later in this section. Additionally, the hydrogen solubility gap at the transformation front is small (about 1 at.%, figure 1), and therefore is neglected in the calculations.

(iii) The dilatometry experiments are assumed to measure the maximum length of the cylinder, although the specimen length may vary along the radial coordinate. This length variation depends on the relative sizes, strengths, and elastic properties of the two Ti phases, as well as their respective hydrogen concentrations. Rather than make assumptions regarding these relationships, we simply take the maximum specimen length to correlate with the maximum hydrogen concentration, since lattice swelling is most pronounced at that point. Therefore, the solutions of equation (2) are evaluated at the radial position corresponding to the maximum hydrogen concentration. During charging, the concentration is a maximum at the cylinder surface ($r = a$, where a is the radius of the cylinder) due to the applied partial pressure. Likewise, the centre of the cylinder ($r = 0$) is evaluated during discharging because the centre of the specimen will retain dissolved hydrogen for the longest time. Errors arising from this assumption will be discussed in a subsequent section.

The discharging of hydrogen from the specimens can then be described using the appropriate solution to equation (2), with a uniform initial concentration and a fixed surface concentration:

$$c(r) = c_{\mathrm{eq}} \quad \text{for } t = 0, \tag{3a}$$

$$c(a) = 0 \quad \text{for } t \geqslant 0. \tag{3b}$$

Experimentally, charging appears to be complete for $t_{\mathrm{c}} \geqslant 600\,\mathrm{s}$ (figure 3), so the above boundary and initial conditions apply for those cases. The appropriate solution is given in Crank (1975) as

$$\frac{c(r,t)}{c_{\mathrm{eq}}} = \frac{2}{a} \sum_{m=1}^{\infty} \frac{\exp\left(-D\alpha_m^2 t\right) J_0(r\alpha_m)}{\alpha_m J_1(a\alpha_m)}, \tag{4a}$$

where $c(r,t)$ is the instantaneous hydrogen concentration, J_n is the Bessel function of the first kind of order n, and α_m are the roots of $J_0(a\alpha) = 0$. Following the assumption stated earlier, for discharging, only the concentration at the centre of the cylinder ($r = 0$) will be considered, for which equation (4a) becomes:

$$\frac{c(0,t)}{c_{\mathrm{eq}}} = \frac{2}{a} \sum_{m=1}^{\infty} \frac{\exp\left(-D\alpha_m^2 t\right)}{\alpha_m J_1(a\alpha_m)}. \tag{4b}$$

In figure 4, the discharging concentration history at the centre of the cylinder ($r = 0$) predicted by equation (4b) is shown as a plot of c/c_{eq} versus t, using both the values of D_α and D_β given above for the hydrogen diffusivity D. For comparison, three sets of dilatometric data for discharging of completely charged cylinders ($t_{\mathrm{c}} = 600, 900,$
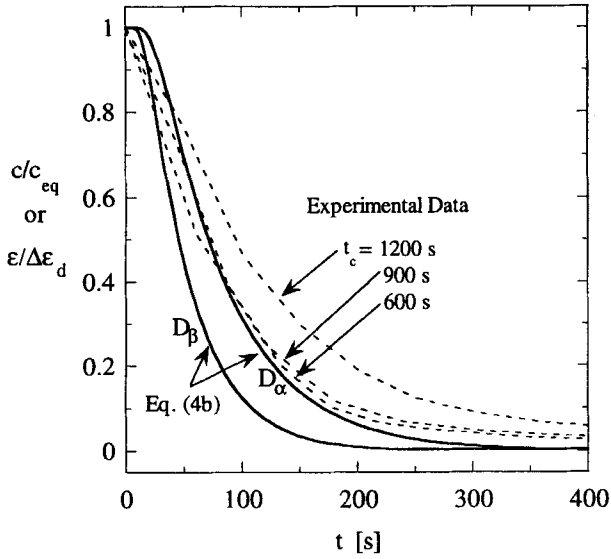
Figure 4. Strain history during hydrogen discharging at 860°C for charging times t_c, normalized by the total discharging strain, $\Delta\varepsilon_d$. Shown for comparison are concentration histories, c/c_{eq}, predicted by equation (4b), using D_α or D_β for the diffusivity of hydrogen in titanium, D.

1200 s) are shown as $\varepsilon/\Delta\varepsilon_d$ versus t, where the instantaneous measured dilatometric strain ε is normalized by the total discharging strain, $\Delta\varepsilon_d$.

In figure 4, the predictions of equation (4b) using D_α and D_β are quite similar, although the predictions using D_α more accurately describe the experimental data. This behaviour may be expected, since diffusion of H out of the cylinder is a serial process of diffusion through β-Ti and α-Ti, with the slower process (diffusion through α-Ti) limiting the kinetics. On charging, however, this limitation is not present. Although $c_{eq} = 16.0$ at.% (equation (1)), the α–β transformation occurs between $c \approx 1$ at.% and $c \approx 2$ at.% (McQuillan 1950). Thus, for most of the charging half-cycle the specimen is entirely in the β-phase, and hydrogen diffusion is controlled by diffusion of H through β-Ti. The kinetics of the phase transformation will be discussed in more detail in a later section.

In figure 4, the reasonable match between the experimental discharging strain histories ($\varepsilon/\Delta\varepsilon_d$ versus t) and the analytical predictions of equation (4b) (c/c_{eq} versus t) suggests that strain and hydrogen concentration may, to a first approximation, be simply proportional:

$$\varepsilon = \Delta\varepsilon_d\left(\frac{c}{c_{eq}}\right). \tag{5}$$

The physical significance of this relationship is explored in the following section.

4.2.1.2. *Lattice swelling strain.* The linear relationship between $\varepsilon/\Delta\varepsilon_d$ and c/c_{eq} (equation (5)) is shown as a dotted line in figure 5, where $\varepsilon/\Delta\varepsilon_d$ is converted to a volume strain by assuming $\Delta V/V = 3\varepsilon$. The slope of this line is equal to the total volume strain on discharging, $(\Delta V/V)(c_{eq}/c) = 3\Delta\varepsilon_d = 0.0156$. As noted in the previous section, this line describes in an approximate manner the relationship
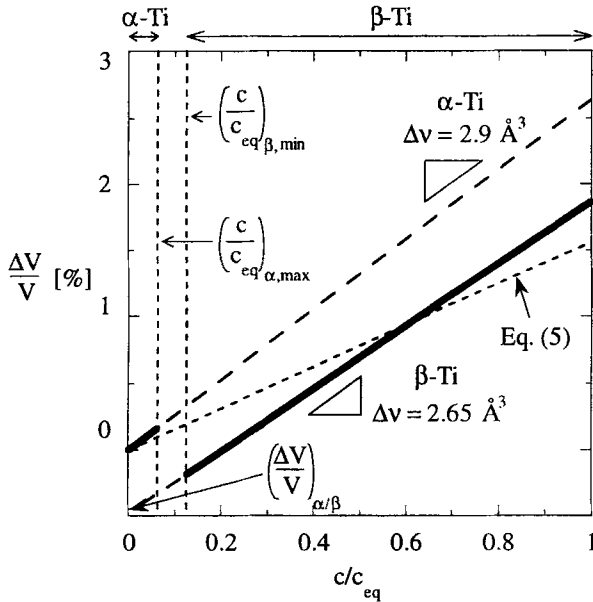
Figure 5.   Volume changes of Ti associated with hydrogen absorption at 860°C. The empirical trend of equation (5) (dotted line) is compared with the theoretical construction (bold line) which accounts for lattice-swelling of both α- and β-Ti, as well as the α–β phase transformation.

between measured dilatometric strain and hydrogen concentration at the centre of the cylinder. This line, however, does not account for the phase transformation which, for the thermal transformation (i.e., without hydrogen), involves a volume shrinkage of $(\Delta V/V)_{\alpha-\beta} = -0.48\%$ (McCoy 1964). In order to physically justify equation (5) as an average relationship, we now consider the volume strains of lattice swelling and the α–β phase transformation from a theoretical perspective.

A theoretical curve describing the $\Delta V/V$ versus c/c_{eq} relationship which accounts for both phase transformation and lattice swelling can be constructed as follows. Lattice swelling upon hydrogen dissolution has been studied in many metals and alloys (Waisman *et al.* 1973, Schober and Wenzel 1978, Gaudett and Scully 1999), for which a linear relationship between volume strain and hydrogen concentration is consistently found:

$$\frac{\Delta V}{V} = \left(\frac{\Delta v}{\Omega}\right) c, \tag{6}$$

where Ω is the atomic volume of the solvent phase, and Δv is the volume of an atom of dissolved H. In the case of α-Ti, $\Omega_\alpha = 17.6\,\text{Å}^3$ (Frost and Ashby 1982) and $\Delta v = 2.9\,\text{Å}^3$ was determined by Waisman *et al.* (1973) at 600°C and 1.5–3.0 at.% H, while for β-Ti, $\Omega_\beta = 18.1\,\text{Å}^3$ (Frost and Ashby 1982) and $\Delta v = 2.65\,\text{Å}^3$ (Waisman *et al.* 1973) from 600°C to 900°C and from 0 to 9.0 at.% H. Using these values and equation (6), the swelling lines for both α- and β-Ti are constructed in figure 5. The line for β-Ti is offset by the volume change during the α → β thermal transformation $(\Delta V/V)_{\alpha/\beta} = -0.48\%$ (McCoy 1964) (in the absence of hydrogen, i.e., at $c/c_{eq} = 0$).

Finally, at 860°C, the hydrogen-induced phase transformation occurs over a narrow range of hydrogen concentrations (figure 1). The two-phase $\alpha + \beta$ field is bounded by the maximum concentration in the α phase, $(c/c_{eq})_{\alpha,max} = 0.063$, and the minimum concentration in the β phase, $(c/c_{eq})_{\beta,min} = 0.13$ (McQuillan 1950). During hydrogen charging or discharging, in which a well-defined concentration gradient is present, the α and β phases cannot coexist between these concentrations, unless the gradient is locally reversed. The full swelling and transformation curve is found by following the swelling trendline for α until $(c/c_{eq})_{\alpha,max}$ is reached, whereupon there is a jump in concentration to $(c/c_{eq})_{\beta,min}$ with an associated transformation shrinkage strain.

The relationship between $\Delta V/V$ and c/c_{eq} described above and shown in figure 5 is constructed solely from literature data and theoretical considerations, with no necessary relationship to the experimental data. However, in comparing the linear relationship of equation (5) (determined from the experimental data) with this constructed curve, it is clear that the average linear relationship is a fair approximation of the more complex behaviour predicted to occur in the specimen.

4.2.1.3. *Hydrogen diffusion during charging.* As previously discussed, ratchetting is assumed to occur only during the charging half of the chemical cycle. Therefore, the measured strain histories on charging (figure 6) comprise contributions from transformation and swelling as discussed in the previous section, plus the plastic deformation of ratchetting. To recover the corrected strain history which would be observed in the absence of ratchetting, the absolute value of the ratchetting strain, $|\Delta\varepsilon_r|$ for each charging time t_c is added to the maximum swelling strain $\Delta\varepsilon_c$ at its respective t_c, as shown in figure 6. This procedure is followed using values of $|\Delta\varepsilon_r|$ acquired from both dilatometric and contact-free experiments, added to $\Delta\varepsilon_c$ measured from the dilatometric experiments.

With the corrected strain histories in figure 6, the kinetics of the charging half-cycles may be analysed in much the same manner as the discharging data were, incorporating the average swelling behaviour described by equation (5) into an appropriate solution to Fick's second law of diffusion (equation (2)). The most physically appropriate solution assumes that the cylinder is initially hydrogen-free ($c(r,0) = 0$ at $t = 0$) and that for $t \geqslant 0$ there is a boundary condition at the cylinder surface:

$$-D\,\frac{\partial c(a,t)}{\partial r} = \mu(c_s - c_{eq}), \tag{7}$$

where c_s is the actual concentration at an infinitesimal depth in the cylinder (Crank 1975). The surface condition above accounts for possible kinetic limitations arising from the dissociation of hydrogen gas ($H_2 \rightarrow 2H$), which occurs in series with the subsequent diffusion process, as noted by for example Gulbransen and Andrew (1949), Laser (1982) and Brown and Buxbaum (1988). The surface-limited mass transfer coefficient μ has units of length/time ($cm\,s^{-1}$), and is left as an adjustable parameter in this analysis. The solution to the diffusion problem with the surface condition of equation (7) is given in Crank (1975) as

$$\frac{c}{c_{eq}} = 1 - \sum_{s=1}^{\infty} \frac{2LJ_0(r\beta_s/a)}{(\beta_s^2 + L^2)J_0(\beta_s)} \exp\left(-\beta_s^2 Dt/a^2\right), \tag{8}$$
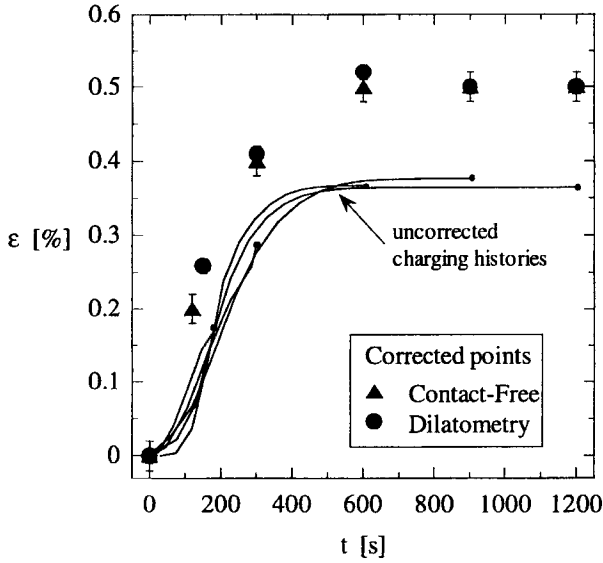
where β_s are the roots of

Figure 6.   Strain history during hydrogen charging at 860°C, including uncorrected, experimental data from figure 2, and data points corrected to remove ratchetting shrinkage. Ratchetting data from both contact-free and dilatometric experiments have been used in the correction.

$$\beta J_1(\beta) - L J_0(\beta) = 0\,, \tag{9}$$

with the dimensionless parameter

$$L = \frac{a\mu}{D}. \tag{10}$$

For charging, as previously assumed, the concentration of interest is at the position $r = a$, and we use D_β for D. Equation (8) can then be simplified and combined with equation (5) to yield

$$\varepsilon = \Delta\varepsilon_{\mathrm{d}} \left[1 - \sum_{s=1}^{\infty} \frac{2L}{(\beta_s^2 + L^2)} \exp\left(-\beta_s^2 Dt/a^2\right) \right]. \tag{11}$$

The predictions of equation (11) are shown in figure 7 for three different surface conditions (three different values of μ). The best fit to the data occurs with $\mu = 5 \times 10^{-4}\,\mathrm{cm\,s^{-1}}$. The predictions are satisfactory for charging times longer than $t_{\mathrm{c}} = 600\,\mathrm{s}$, with some error for shorter times. The origin of the error is most probably in the use of D_β to describe diffusion; for short charging times the specimen retains some α phase, which tends to slow hydrogen diffusion into the cylinder.

The dimensionless parameter L (equation (10)) is analogous to the convection coefficient (i.e., Biot number) in heat transfer problems (Livanov *et al.* 1965, Makhlouf and Sisson 1991); L values near zero indicate that diffusion is kinetically limiting. In the present case, with the best-fit value $\mu = 5 \times 10^{-4}\,\mathrm{cm\,s^{-1}}$, $L \approx 0.72$, which indicates that the surface condition plays a large role in determining the charging kinetics. This is consistent with prior reports on the diffusion of gaseous hydrogen into various metals, and is associated with molecular hydrogen dissociation (Gulbransen and Andrew 1949, Louthan and Derrick 1975, Fromm and Wulz
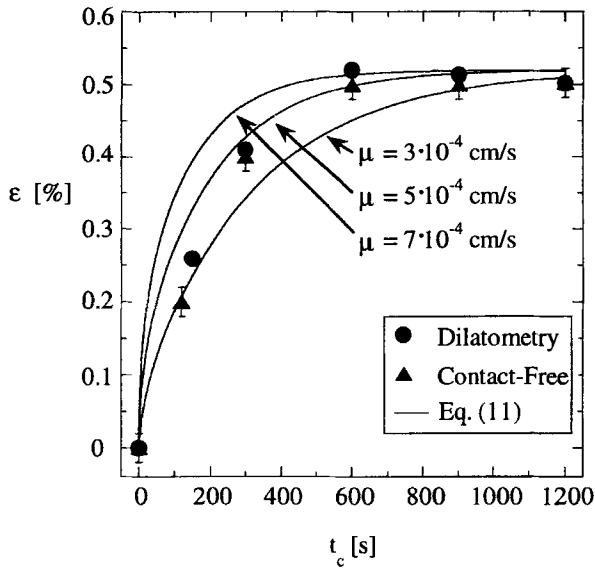
Figure 7. Corrected charging strains from figure 6 (with same symbols as in that figure), compared with the analytical predictions of equation (11) with different surface conditions, μ.

1984, Wulz *et al.* 1986, Makhlouf and Sisson 1991, Lewkowicz 1996, Viano *et al.* 1998), although no value for μ was found in the literature for Ti.

4.2.2. *Chemical ratchetting*

Having established the utility of simple diffusion equations to describe the strain evolution both on discharging (equation (4)) and charging (equations (8) and (11)), these equations can now be used to determine the radial position $r_{\alpha-\beta}$ of the $\alpha-\beta$ transformation front at any time. Taking the transformation front to occur at $(c/c_{eq})_{\alpha,max} = 0.0625$, the value of $r_{\alpha-\beta}$ is given implicitly by equation (8) on charging and equation (4*a*) on discharging. Figure 8 shows $r_{\alpha-\beta}$ predicted by these equations as a function of time for both charging (with $\mu = 5 \times 10^{-4}$ cm s^{-1}) and discharging. Although this analysis is approximate and involves many simplifying assumptions, figure 8 illustrates that complete $\alpha \rightarrow \beta$ transformation of the cylinder is expected after only about 45 s of charging, while on discharging, the $\beta \rightarrow \alpha$ reversion requires about 200 s. By contrast, charging to full hydrogen content ($c/c_{eq} = 1$) requires about 600 s as determined experimentally and verified by equation (11) (figure 7). Furthermore, the ratchetting strain, $|\Delta\varepsilon_r|$ increases monotonically between $t_c = 0$ and 600 s (figure 3).

It follows from the above analysis that the $\alpha \rightarrow \beta$ transformation was probably complete for all of the experiments performed, since the shortest non-zero charging time investigated was $t_c = 120$ s. Therefore the increasing ratchetting strain measured for longer charging times ($t_c > 120$ s) is caused solely by the swelling of the β phase, without additional phase transformation. Since the β phase is cubic, anisotropy due to crystallographic texture is not expected to constitute a significant contribution. From these observations, we conclude that strain gradients due to β-lattice swelling contribute to chemical ratchetting independently of the $\alpha-\beta$ phase transformation.
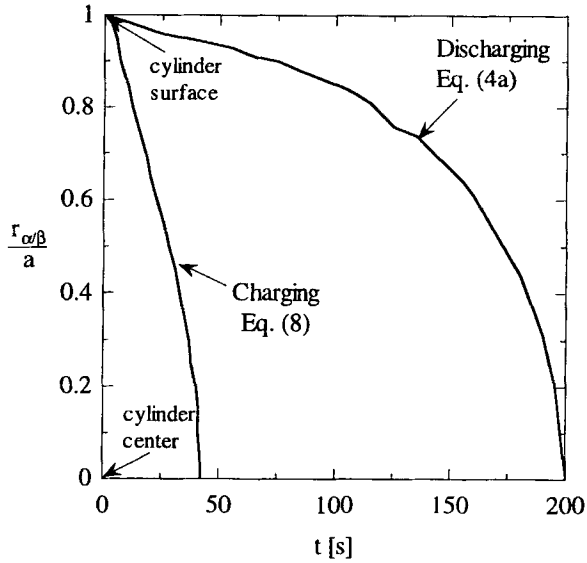
Figure 8. Radial position of the α–β phase transformation front during both charging and discharging at 860°C, as given by equations (8) and (4 a), respectively.

This conclusion is supported by the chemical cycling experiment performed at 1000°C in the β-phase (figure 1), which involved no phase transformation but still resulted in a ratchetting strain of $\Delta\varepsilon_r = -0.07\%$ after a single cycle. This result may have significant implications for hydrogen storage in non-allotropic metals, in which hydrogen is cyclically added and removed for use as a fuel (Viano *et al.* 1998, Li and Wang 1999a,b). Although the chemical ratchetting strains measured in the present study are small, repeated cycling may result in their accumulation, leading to large macroscopic deformation as observed in thermal ratchetting (Buckley *et al.* 1958, Stobo 1960). Furthermore, these results demonstrate that chemical ratchetting may occur with or without an associated phase transformation.

§ 5. CONCLUSIONS

We have investigated the macroscopic deformation of titanium during its α–β transformation without externally applied stress (i.e., ratchetting). Experiments involved either (a) thermally cycling about the allotropic temperature of 882°C, or (b) chemically cycling the composition by the introduction and removal of hydrogen gas at 860°C to induce the α–β transformation. The major results of this study are summarized here.

(a) Thermal cycling of extruded (i.e., textured) titanium about its α–β transformation temperature produces an irreversible elongation of the specimens in the extrusion direction by 0.05%.

(b) Chemical cycling of titanium by alloying and dealloying with hydrogen at 860°C and $P_{H_2} = 38.7$ Torr to trigger the α–β transformation produced ratchetting shrinkage strains of at most −0.15% after a single cycle.

(c) A simplified description of hydrogen diffusion is sufficiently accurate to describe the kinetics of strain evolution during hydrogen discharging. This

approach is further adapted to the case of charging by the incorporation of a surface condition, arising from the $H_2 \rightarrow 2H$ decomposition.

(d) Kinetic analysis shows that specimens are fully transformed (α–β) in 45 s, about one-tenth the experimental time for full charging. The ratchetting strains therefore evolve during the α–β phase transformation, and also after the transformation is complete, due to internal stresses arising from lattice swelling in β-Ti.

REFERENCES

BAILEY, J. E., 1963, *Acta metall.*, **11**, 267.
BALASUBRAMANIAM, R., 1993, *Acta metall.*, **41**, 3341.
BIRNBAUM, H. K., GROSSBECK, M. L., and AMANO, M., 1976, *J. less-common Metals*, **49**, 357.
BREE, J., 1967, *J. Strain Anal.*, **2**, 226.
BROWN, C. C., and BUXBAUM, R. E., 1988, *Metall. Trans.*, **19A**, 1425.
BUCKLEY, S. N., HARDING, A. G., and WALDRON, M. B., 1958, *J. Inst. Metals.*, **87**, 150.
BURKE, J. E., and TURKALO, A. M., 1952, *J. Metals.*, **4**, 651.
CRANK, J., 1975, *The Mathematics of Diffusion* (Oxford: Clarendon Press).
EARMME, Y. Y., JOHNSON, W. C., and LEE, J. K., 1981, *Metall. Trans.*, **12**, 1521.
FROES, F. H., and EYLON, D., 1990, *Hydrogen Effects of Material Behaviour*, edited by N. R. Moody and A. W. Thompson (Warrendale, PA: The Minerals, Metals and Materials Society), p. 261.
FROMM, E., and WULZ, H. G., 1984, *J. less-Common Metals*, **101**, 469.
FROST, H. J., and ASHBY, M. F., 1982, *Deformation Mechanism Maps* (Oxford: Pergamon Press).
FURUSHIRO, N., KURAMOTO, H., TAKAYAMA, Y., and HORI, S., 1987, *Trans. Iron Steel Inst. Jap.*, **27**, 725.
GAUDETT, M. A., and SCULLY, J. R., 1999, *Metall. Mater. Trans.* A, **30**, 65.
GREENWOOD, G. W., and JOHNSON, R. H., 1962, *React. Sci. Technol.*, **16**, 473.
GULBRANSEN, E. A., and ANDREW, K. F., 1949, *Trans. AIME*, **185**, 741.
HALL, I. W., and PATTERSON, W. G., 1991, *Scripta Mater.*, **25**, 805.
LAMPMAN, S., 1990, *ASM Handbook: Properties and Selection: Nonferrous Alloys and Special Purpose Materials* (Metals Park, OH: ASM International), p. 614.
LASER, D., 1982, *J. Vacuum Sci. Technol.*, **20**, 37.
LEE, J. K., EARMME, Y. Y., AARONSON, H. I., and RUSSELL, K. C., 1980, *Metall. Trans.*, **11**, 1837.
LEWKOWICZ, I., 1996, *Solid State Phenomena*, Vol. 50, edited by F. A. Lewis and A. Aladjem (Vaduz, Liechtenstein: Scitec Publications), p. 239.
LI, C.-J., and WANG, X.-L., 1999a, *J. Alloys Compounds*, **284**, 270.
LI, C.-J., and WANG, X.-L., 1999b, *J. Alloys Compounds*, **284**, 274.
LIVANOV, V. A., BUKHANOVA, A. A., and KOLACHEV, B. A., 1965, *Hydrogen in Titanium* (New York: Daniel Davey).
LOUTHAN, M. R., and DERRICK, R. G., 1975, *Corrosion Sci.*, **15**, 565.
MAKENAS, B. J., and BIRNBAUM, H. K., 1980, *Acta metall.*, **28**, 979.
MAKHLOUF, M. M., and SISSON, R. D., 1991, *Metall. Trans.*, **22**, 1001.
McCOY, H. E., 1964, *Trans. Amer. Soc. Metals*, **57**, 743.
McQUILLAN, A. D., 1950, *Proc. R. Soc. Lond.* A, **204**, 309.
NAKANISHI, M., NISHIDA, Y., MATSUBARA, H., YAMADA, M., and TOZAWA, Y., 1990, *J. Mater. Sci. Lett.*, **9**, 470.
PATON, N. E., HICKMAN, B. S., and LESLIE, D. H., 1971, *Metall. Trans.*, **2**, 2791.

PONTER, A. R. S., and COCKS, A. C. F., 1984, *J. appl. Mech.*, **51**, 470.

PULS, M. P., 1981, *Acta Metall.*, **29**, 1961.

SCHOBER, T., 1973, *Scripta Metall.*, **7**, 1119.

SCHOBER, T., and WENZEL, 1978, *Hydrogen in Metals*, Vol. II, edited by G. Alefeld and J. Volkl (Berlin: Springer-Verlag), p. 11.

SENKOV, O. N., JONAS, J. J., and FROES, F. H., 1996, *JOM*, **48**, 42.

STOBO, J. J., 1960, *J. nucl. mater.*, **2**, 97.

VIANO, A. M., MAJZOUB, E. H., STROUD, R. M., KRAMER, M. J., MISTURE, S. T., GIBBONS, P. C., and KELTON, K. F., 1998, *Phil. Mag. A*, **78**, 131.

WAISMAN, J. L., SINES, G., and ROBINSON, L. B., 1973, *Metall. Trans.*, **4**, 291.

WASILEWSKI, R. J., and KEHL, G. L., 1954, *Metallurgia*, **50**, 225.

WULZ, H. G., CICHY, H., and FROMM, E., 1986, *J. less-Common Metals*, **118**, 303.

YOUNG, A. G., GARDINER, K. M., and ROTSEY, W. B., 1960, *J. nucl. mater.*, **2**, 234.

ZWIGL, P., and DUNAND, D. C., 1998, *Metall. Mater. Trans.*, **29A**, 565.